

Myosin-I Isozymes in Neonatal Rodent Auditory and Vestibular Epithelia

RACHEL A. DUMONT,¹ YI-DONG ZHAO,² JEFFREY R. HOLT,³ MARTIN BÄHLER,⁴ AND PETER G. GILLESPIE¹

¹Oregon Hearing Research Center and Vollum Institute, Oregon Health & Science University, Portland, OR 97201, USA

²Department of Physiology, Johns Hopkins University, Baltimore MD 21205, USA

³Harvard Medical School and Massachusetts General Hospital, Boston MA 02114, USA

⁴Institut für Allgemeine Zoologie und Genetik, Westfälische Wilhelms-Universität Münster, Münster, Germany

Received: 22 October 2001; Accepted: 18 December 2001; Online publication: 27 February 2002

ABSTRACT

Myosin isozymes are essential for hair cells, the sensory cells of the inner ear. Because a myosin-I subfamily member may mediate adaptation of mechano-electrical transduction, we examined expression of all eight myosin-I isozymes in rodent auditory and vestibular epithelia. Using RT-PCR, we found prominent expression of three isozymes, Myo1b (also known as myosin-I α or myr 1), Myo1c (myosin-I β or myr 2), and Myo1e (myr 3). By contrast, Myo1a (brush-border myosin-I), Myo1d (myosin I γ or myr 4), Myo1f, Myo1g, and Myo1h were less readily amplified. Because sequence analysis demonstrated that the RT-PCR products encoded the appropriate isozymes, this represents the first demonstration of expression of all eight mouse myosin-I genes. Using immunocytochemistry with isozyme-selective antibodies, we found that Myo1b was located at apical surfaces of supporting cells that surround hair cells in auditory epithelia of postnatal rats. In vestibular epithelia, Myo1b was present in a ring within the apical pole of the hair cell. In both cases, expression was prominent only immediately after birth. Myo1e was found in hair cells of the auditory and vestibular epithelia; this isozyme was enriched in the cuticular plate, the actin meshwork that anchors the stereocilia. Myo1c was found in

hair-cell stereocilia, concentrated towards their tips; we confirmed this localization by using adenovirus vectors to direct expression of a GFP-Myo1c tail fusion protein; this fusion protein localized to plasma membranes, often concentrating at stereociliary tips. Myo1c therefore remains the myosin isozyme best localized to carry out transducer adaptation.

Keywords: myosin, hair cells, stereocilia, adaptation, transduction

INTRODUCTION

Hair cells, the sensory cells of the auditory and vestibular systems, rely on actin-rich structures for mechano-electrical and electromechanical transduction (Gillespie et al. 1996). The mechanically sensitive hair, bundle is largely made up of stereocilia, which consist of highly crosslinked, parallel actin filaments enveloped by plasma membrane. Stereocilia insert into and are anchored by the cuticular plate, a meshwork of randomly oriented actin filaments (DeRosier and Tilney 1989). Circumferential actin rings in hair cells and supporting cells may contribute to the stiffness of the apical epithelial surface (Drenckhahn et al. 1991). Finally, cortical actin filaments are essential for the specialized contractile activity of the outer hair cell's lateral wall (Holley et al. 1992).

The prominence of actin-containing structures within hair cells suggests that motor proteins that generate force along actin will also prove essential for proper function of these sensory cells. Indeed, mu-

Correspondence to: Peter G. Gillespie, Ph.D. • Oregon Hearing Research Center & Vollum Institute • L335A / Oregon Health & Science University • 3181 SW Sam Jackson Park Road • Portland, OR 97201. Telephone: (503) 494-2936; fax: (503) 494-2976; email: gillespp@ohsu.edu

TABLE 1

Myosin-I nomenclature			
Name	Other names	GenBank accession numbers	PCR primers
Myo1a	Brush-border Myosin-I	AF009960	(+) 5'-CTACAGCAGGTGTTTCATAG-3' (-) 5'-TGGAAACAAGGACTTCAGG-3'
Myo1b	Myosin-l α ; myr 1; MI-130K	NM_010863	(+) 5'-CAAGAGGTGAAAGAACTTC-3' (-) 5'-TCTTCGTTCAACTGTTCCGG-3'
Myo1c	Myosin-l β ; myr 2; MI-110K	NM_008659	(+) 5'-AGTCTCTGTCAATCCCTACC-3' (-) 5'-GGAGGTAAGTGAATGTGG-3'
Myo1d	Myosin-l γ ; myr 4	BF016443	(+) 5'-GCAGAAGTCACTCTCATCC-3' (-) 5'-CTTGCCAAAGGGCTCTCTG-3'
Myo1e	Myr 3	AA250515; BF016461; BG076620; BG086565	(+) 5'-CAAGAAGCCTAAAGACTGGG-3' (-) 5'-TCCTCCTCTCCTTCTGTTC-3'
Myo1f		NM_008660	(+) 5'-CTACATACCCTCCCTCACC-3' (-) 5'-TCCCCACACGACACCTTG-3'
Myo1g		BE848707; AW986090;	(+) 5'-ACTAAAGGCACCTTCGGGAG-3' (-) 5'-GGCTCCACAGAAATGAGGC-3'
Myo1h		AK014505	(+) 5'-AGTTCGTAGTCTGTGAGG-3' (-) 5'-GTATGCTGACCTCTGTGTG-3'

^aNote that there is confusion in the literature and databases between Myo1c and Myo1e. We use the mouse names for the rat isozymes as well. GenBank accession numbers refer to complete sequences (Myo1a, Myo1b, Myo1c, Myo1f) or ESTs used in characterization of other isozymes (Myo1d, Myo1e, Myo1g, Myo1h).

tations in at least four myosin genes of humans or mice—*MYH9*, *MYO6*, *MYO7a*, and *MYO15*—lead to deafness and vestibular dysfunction (Avraham et al. 1995; Gibson et al. 1995; Probst et al. 1998; Lalwani et al. 2000). Other myosin isozymes may be necessary for hair cells; indeed, the full complement of myosin isozymes required by hair cells remains unknown. An RT-PCR screen identified 13 myosin isozymes, from six separate classes, in the frog saccule (Sole et al. 1994). Other myosin isozymes known to be expressed in rodent hair-cell epithelia were not detected in this PCR screen, however, including Myo15 (Probst et al. 1998) and Myo1f (Crozet et al. 1997). Other members of the myosin-I class were, however, prominent in this screen.

Myosin-I isozymes are 100–130 kD and share several structural features, including an actin- and ATP-binding head domain, a neck region containing one to six calmodulin-binding IQ domains, and a highly basic tail that mediates interaction with acidic phospholipids (Coluccio 1997). One member of this class, myosin-1c (Myo1c; formerly known as myosin-1 β ; see Table 1 and nomenclature note in Materials and Methods), may facilitate adaptation of mechano-electrical transduction (Gillespie and Corey 1997). Localization and biochemical data support this suggestion in the bullfrog sacculus. Myo1c is located at stereociliary tips, near the end of tip links (Gillespie et al. 1993; Hasson et al. 1997; Garcia et al. 1998; Steyger et al. 1998). A 120-kD protein that can be photoaffinity labeled with radioactive nucleotides has pharmacological properties consistent with those of the adaptation motor (Gillespie et al. 1993; Yamoah and Gillespie 1996; Burlacu et al. 1997); the strongest

candidate for this photolabeled protein is Myo1c. Finally, adaptation can be blocked by a mutant-selective inhibitor when a mutant Myo1c is expressed in mouse hair cells (Holt et al. 2002).

Because of the powerful transgenic and gene-targeting techniques available for analysis of gene function in mice, rodents are more amenable to testing the role of specific proteins in hair-cell function. In addition, adenovirus-mediated gene transfection has proven successful in mouse hair cells (Holt et al. 1999). Fortunately, mechano-electrical transduction in mouse vestibular hair cells resembles closely that in more thoroughly characterized frog hair cells (Holt et al. 1997). These techniques should in the future permit more rigorous testing of hypotheses for roles for myosin molecules in these cells.

Although Myo1c is the best candidate for the frog saccule adaptation motor, other myosin-I isozymes might contribute to the motor. Therefore, we sought to document the locations of members of the myosin-I family in the rodent auditory and vestibular systems. We found that three myosin-I isozymes, Myo1b, Myo1c, and Myo1e, are expressed at birth in cochlea and vestibular organs, but only Myo1c remains at a high level subsequently. Localization at stereociliary tips confirms that Myo1c is a strong candidate for the adaptation-motor myosin of rodent vestibular hair cells.

METHODS

Myosin nomenclature

Nomenclature for myosin-I isozymes is confusing and contradictory (Berg et al. 2001). Although several

names have been used for each of the myosin isozymes examined here, we adopt here the official Human Genome Organization (HUGO) names (<http://www.gene.ucl.ac.uk/nomenclature/>; Table 1). This nomenclature has been adopted by almost all researchers studying vertebrate myosin-I isozymes (Gillespie et al. 2001).

RT-PCR

Purified total RNA (RNeasy Kit, Qiagen, Valencia, CA) from P3–P12 mouse utricles was primed using random hexamers and reverse-transcribed (ThermoScript RT-PCR System, Life Technologies, Carlsbad, CA). Isozyme-specific primers (Table 1) were used in PCR reactions to detect each myosin-I. The amplification protocol with Taq polymerase (Promega, Madison, WI) comprised 4 min at 94°C, 25–30 cycles of 60 s at 94°C, 30 s at 50°C, 50 s at 72°C, and a final 10 min at 72°C. The amplification protocol with a proofreading polymerase (Proofstart, Qiagen) comprised 5 min at 95°C, 35 cycles of 60 s at 94°C, 30 s at 50°C, 50 s at 72°C, and a final 10 min at 72°C. PCR products were cloned into the pCR2.1-TOPO vector (TOPO Cloning, Invitrogen, Carlsbad, CA). Cloned PCR products were sequenced using the vector M13 reverse primer or T7 promoter primer.

Hair-bundle purification

This method was similar to those described for frog saccular and utricular hair bundles (Gillespie and Hudspeth 1991; Steyger et al. 1998). Rat or mouse vestibular organs were dissected in minimal essential medium (MEM, Life Technologies), which was supplemented with 25 mM HEPES pH 7.5, and were adhered to a coverslip coated with Cell-Tak (Becton Dickinson Labware, Bedford, MA). Molten low-melting-point agarose (3%–4% in MEM) at 37°C was used to flood the coverslip, then was allowed to set to a firm gel by cooling to 4°C. Bundles were severed from hair-cell bodies by shearing the agarose relative to the coverslip. Under dark-field illumination, bundles were visualized and excised in a plug of agarose.

Protein purification

Production of rat Myo1c in baculovirus has already been described (Gillespie et al. 1999); the resulting protein has an N-terminal hexahistidine tag, which is used for purification. Myo1b (b splice form) was introduced into the pVL1392 baculovirus transfer vector; Myo1e was introduced into pVL1393. Both constructs encoded full-length myosin molecules without epitope tags. Recombinant baculoviruses were produced using standard techniques (O'Reilly

et al. 1994). Myo1b, Myo1c, and Myo1e were expressed by infecting Sf9 insect cells with recombinant baculoviruses. In a typical experiment, $4\text{--}8 \times 10^8$ Sf9 cells in 400 mL of Grace's medium (Life Technologies) containing 3.3 mg/mL lactalbumin hydrolysate, 3.3 mg/mL yeastolate, 20 $\mu\text{g}/\text{mL}$ gentamicin, 0.1% Pluronic F-68, and 10% fetal calf serum were infected with myosin and calmodulin viruses at a multiplicity of infection of 4 and 2, respectively. After 48 h at 27°C, the cells were centrifuged at 1500g, washed with PBS, and recentrifuged. Pelleted cells were stored at -80°C prior to use. For purification, cells were thawed, resuspended with purification buffer (25 mM Tris pH 7.5, 0.5 mM MgCl_2 , 0.5 mM EGTA, 2.5 mM 2-mercaptoethanol, 0.2 mM PMSF, 1 μM leupeptin, 1 μM pepstatin), and lysed by passage through 22 gauge and 25 gauge needles. The lysate was adjusted to 300 mM NaCl and 1 mM ATP and was centrifuged at 400,000 g for 30 min. Myo1c was purified by Ni^{2+} -NTA affinity chromatography and gel filtration as described (Gillespie et al. 1999).

For other isozymes, the supernatant was diluted to a NaCl concentration of 100 mM (Myo1b) or 150 mM (Myo1e) and was loaded on to a HiTrap SP cation-exchange column (Amersham Pharmacia Biotech). After washing with isolation solution containing the same NaCl concentration, bound proteins were eluted with a salt gradient. Myosin-containing fractions were identified by immunoblotting. Purified actin, stabilized with an equimolar concentration of unlabeled phalloidin, was added to a final concentration of 5 μM ; after incubation on ice for 30 min, the solution was centrifuged at 400,000 g for 30 min. After resuspending the actomyosin pellet with 1 mM ATP, 50 mM KCl, 1 mM MgCl_2 , 0.1 mM EGTA, and 15 mM HEPES at pH 7.5, the solution was recentrifuged at 400,000 g for 30 min. Myo1b or Myo1e were found in the supernatant fluid at 25–50% purity; we estimated their concentrations by densitometry using BSA as a standard.

Protein immunoblots

For quantitation of myosin-isozyme levels in rat inner-ear organs, both vestibular organs and segments of cochlea were dissected from 3–4-day-old pups, treated with SDS-containing sample buffer, and analyzed by protein immunoblotting as described (Gillespie and Gillespie 1997; Hasson et al. 1997). Standards of partially purified (Myo1b, Myo1e) or purified (Myo1c; Gillespie et al. 1999) myosin were included on the immunoblots for quantitation. Myo1c in mouse hair bundles and residual maculae (the epithelium remaining after hair-bundle isolation) was measured similarly; actin was detected using an IgM monoclonal antibody (N350; Amersham Pharmacia

Biotech, Piscataway, NJ) that recognizes all actin isoforms. Purified platelet actin (Cytoskeleton, Denver, CO), a mixture of 85% β -actin and 15% γ -actin, was used as a standard for immunoblotting.

Myosin antibodies

Affinity-purified antibodies against Myo1b (Tü 30), Myo1d (Tü 12), and Myo1e (FML 6) have been described previously (Ruppert et al. 1993; Bähler et al. 1994; Stoffler et al. 1995). Myo1c antisera directed against either the C-terminal 15-kD or 30-kD domain of rat Myo1c were produced for this study. Using primers for rat Myo1c (15 kD forward—CAGGGA TCCAAGCCTCGTCCCGGCAG, 30 kD forward—CAGGGATC-CATTTTGGCGTCATGCACCCC, reverse CAGTGCAAGCTTTCATCACCGAGAATTCAGCC) that introduced *Bam* H I and *Hind* III restriction-endonuclease sites, we amplified by PCR segments of rat Myo1c cDNA corresponding to amino acids 899–1028 or 760–1028 of rat Myo1c. Fragments were cloned into pET-28a(+) (Novagen, Madison, WI), introducing a hexahistidine tag. Following expression in *E. coli* strain BL21(DE3), 15-kD or 30-kD fragments (His₆-R15 and His₆-R30) were purified on Ni²⁺-NTA (Qiagen) in the presence of 6 M urea. After dialysis against PBS, insoluble His₆-R15 or His₆-R30 were used separately to immunize rabbits (Covance Research Products, Denver, PA).

The R2652 antiserum, raised against His₆-R15, was affinity purified against the C-terminal 30-kD domain of Myo1c, fused to glutathione-S-transferase (GST-R30). To generate GST-R30, PCR was used to amplify a cDNA fragment corresponding to amino acids 760–1028 of rat Myo1c cDNA using the primers described above. The PCR product was cloned into the pGEX-6p-l vector (Amersham Pharmacia Biotech). GST-R30 was expressed in BL21(DE3) cells, extracted from the cell pellet with 6 M urea, dialyzed against 2 M urea/PBS, and purified on a glutathione-agarose column in the presence of 2 M urea. After elution with 2.5 M urea, 15 mM glutathione, 5 mM DTT, and 1.5% octyl glucoside in PBS, the fusion protein was dialyzed against 2 M urea/PBS, then coupled to Affi-Gel 10 (Bio-Rad, Hercules, CA) in the presence of 2 M urea. R2652 antiserum was passed over this column; after washing, the column was sequentially eluted with 100 mM glycine (pH 2.5) and 100 mM 3-[cyclohexylamino]-1-propanesulfonic acid (pH 11). Eluted antibodies were dialyzed against PBS prior to use.

The R2695 antiserum, raised against His₆-R30, was affinity purified as above against a baculovirus-expressed tail construct incorporating amino acids 701–1028 of rat Myo1c (J. Cyr, R.A.D., and P.G.G, unpublished data), which was coexpressed with calmodulin and coupled to CNBr-Sepharose (Amersham Pharmacia Biotech).

Immunofluorescence microscopy

Vestibular epithelia and segments of cochlea were dissected from P1 (i.e., one-day postnatal), P7, P14, or P21 rat pups, fixed with 3% formaldehyde in MEM (Life Technologies), and permeabilized with 0.2% saponin. Following blocking and permeabilization with 5% goat serum, 1% BSA, and 0.1% saponin for 60 min, tissues were incubated overnight at 4°C with primary antibodies in 1% goat serum, 1% BSA, and 0.1% saponin. After washing, biotin-conjugated goat antirabbit antibodies (6 μ g/mL; Vector Laboratories, Burlingame, CA) were applied for 60 min at room temperature. After washing, bound antibodies were detected by incubation with 5 μ g/mL Cy5-streptavidin (Jackson ImmunoResearch Labs, West Grove, PA) and 0.4 μ M FITC-phalloidin (Sigma-Aldrich, St. Louis, MO) for 60 min. For some experiments, detection with the R2652 antiserum against Myo1c employed an amplification method (Adams 1992) between the latter two steps. Following the secondary antibody incubation, tissues were treated with HRP-labeled streptavidin. Treatment with biotinylated tyramine and H₂O₂ permitted deposition of polymerized biotinylated tyramine, which was detected with Cy5-streptavidin. As above, tissues were counterstained with FITC-phalloidin. Bound antibodies were observed using Zeiss LSM 410 or Bio-Rad MRC 1024 confocal microscopes and a 60X or 100X, 1.4 numerical aperture oil-immersion lens.

Adenovirus production and use

Replication-deficient (E1a/b deleted) recombinant adenovirus was generated as previously described (Holt et al. 1999). For this study, DNA encoding the enhanced green fluorescent protein (EGFP) was fused in frame to DNA encoding the tail portion of Myo1c (residues 698–1028) and was inserted into the multiple cloning site of an adenovirus shuttle plasmid immediately downstream of the cytomegalovirus promoter. The shuttle plasmid was cotransfected with a plasmid that carried the adenovirus genome into BJ5183 cells to yield pAdGFP::T698. The plasmid was transfected into and virus was serially amplified in E1-transformed HEK 293 cells. The virus was then purified by density centrifugation on CsCl gradients to yield a stock titer of 4×10^{10} particles/ml of pAdGFP::T698.

The sensory epithelia of P2 mice were removed and grown in organotypic culture for 36–48 h as previously described (Holt et al. 1997, 1999). Epithelia were exposed to 4×10^8 particles/ml pAdGFP::T698 for 24 h. Twelve to 24 h later, epithelia were fixed and counterstained with rhodamine-conjugated phalloidin. The samples were imaged on a Bio-Rad MRC 1024 confocal microscope.



Fig. 1. RT-PCR analysis of mouse utricle myosin-I mRNA. Total RNA was isolated from mouse utricles and cDNA was prepared by reverse transcription. Isozyme-specific primers were used to amplify cDNAs corresponding to each myosin-I. The negative control substituted water for cDNA; rat PMCA2 primers were used for a positive control reaction (not shown). PCR was carried out using Taq polymerase for 25 cycles (top) or 30 cycles (bottom). Although we did not observe Myo1a and Myo1g products in these reactions, they were detected in several other experiments.

RESULTS

RT-PCR

To identify myosin-I isozymes in rodent inner ears, we examined mRNA expression using RT-PCR. The human genome contains eight myosin-I genes in four subgroups (Berg et al. 2001; see Table 1); we assumed that the mouse genome contains orthologs for each isozyme. Full-length sequences for four of these isozymes (Myo1a, Myo1b, Myo1c, and Myo1f) have been cloned from mouse tissues (Sherr et al. 1993; Crozet et al. 1997; Skowron and Mooseker 1999). To identify mouse DNA segments encoding the other four myosin isozymes, we used the BLAST search algorithm (Altschul et al. 1990) to search the database of mouse expressed sequence tags (ESTs). Using rat (Myo1d, Myo1e) or human (Myo1g, Myo1h) query sequences, we identified at least one mouse EST for each myosin-I not already cloned from mouse (Table 1). In some cases, we used overlapping ESTs to construct a partial contiguous sequence. Using these sequences, we designed primers with similar melting temperatures that amplified similar-sized products from each of the myosin-I isozymes under identical conditions, then demonstrated using control tissues that each primer pair successfully amplifies the appropriate sequence (not shown). To ensure that we did not amplify genomic DNA, we confirmed from the partially complete mouse genome sequence (http://mouse.ensembl.org/Mus_musculus/blastview) for Myo1c, Myo1d, Myo1f, and Myo1g that our PCR products spanned introns; genomic products would have been substantially larger than the products we predicted and detected. Although genomic sequence is not yet available for Myo1a, Myo1b, Myo1e, or Myo1h, the regions amplified span introns in the homologous human sequences (<http://www.ncbi.nlm.nih.gov/genome/seq/HsBlast.html>). If the intron-exon boundaries are conserved between mouse and hu-

man, as is likely, genomic products should also be distinguishable from cDNA products in these PCR reactions.

Using these isozyme-selective primers, we carried out RT-PCR on cDNA derived from neonatal mouse utricle. In 25-cycle reactions with Taq polymerase, we observed prominent PCR products for Myo1b, Myo1c, and Myo1e (Fig. 1). Extension of the PCR to 30 or more cycles reproducibly led to successful amplification of Myo1d and Myo1f, and sometimes amplified Myo1a, Myo1g, and Myo1h. Although not quantitative, these results suggest that Myo1b, Myo1c, and Myo1e are expressed at higher levels than are other myosin-I isozymes.

With one exception (Myo1a), we amplified myosin-I fragments for sequencing in two separate experiments, one with Taq polymerase and one with a proofreading polymerase (Fig. 2). Although Myo1a was amplified with only Taq polymerase, the sequence we obtained was identical to that in GenBank (AF009960). For all other isozymes, we obtained identical sequences with both polymerases from different cDNA preparations. Although amplified products from Myo1c were identical to the corresponding mouse sequence in GenBank (NM_008659), Myo1b and Myo1f products differed significantly from mouse sequences in GenBank. Our Myo1b sequence differed in 8 positions from that of the GenBank entry (NM_010863), producing substantial changes in the predicted amino acid sequence. Five nucleotide differences and three inserted nucleotides between nucleotides 1107 and 1148 in the GenBank sequence predict a very different amino acid sequence for NM_010863 (IELNEKFASRPASVK for residues 304–318) than for our entry (NELKEICELTSIDQ). The amino acid sequence of rat Myo1b (X68199) is identical to our predicted sequence in this region, however, suggesting that our sequence is representative. Our Myo1f sequence differed in 16 positions from that of the GenBank entry (NM_008660), producing five changes in the predicted amino acid sequence. Only one of the amino acid changes was conservative. Two of the nucleotide changes that did not alter the amino acid sequence were found in at least one EST but not others (nucleotides 206 and 215 of NM_008660), suggesting that they are polymorphisms. All of the remaining 14 discrepant nucleotides where our sequence differed from NM_008660 were identical to the corresponding nucleotides in all other ESTs we found (not shown), suggesting that our sequence is representative.

Other than EST sequences, no mouse nucleotide sequences are available for Myo1d, Myo1e, Myo1g, and Myo1h. At the amino acid level, our Myo1d product was 99% identical to a mouse Myo1d amino acid sequence (myosin-I γ ; C45438) and 99%

Myo1b

mMyo1b RT-PCR	-----VFYQLLSGASEELLKYLKLERDFSRYNYLSLDSA	34
mMyo1b	GERNFHVVFYQLLSGASEELLKYLKLERDFSRYNYLSLDSA	240
mMyo1b	GERNFHVVFYQLLSGASEELLKYLKLERDFSRYNYLSLDSA	240
mMyo1b RT-PCR	KVNGVDDAANFRVTRNAMQI VGF LDHEAEAVLEVVAAVLK	74
mMyo1b	KVNGVDDAANFRVTRNAMQI VGF LDHEAEAVLEVVAAVLK	280
mMyo1b	KVNGVDDAANFRVTRNAMQI VGF LDHEAEAVLEVVAAVLK	280
mMyo1b RT-PCR	LGNIEFKPESRVNGLDESKIKDKNELKE-ICELTSIDQVV	113
mMyo1b	LGNIEFKPESRVNGLDESKIKDKNELKE-ICELTSIDQVV	320
mMyo1b	LGNIEFKPESRVNGLDESKIKDKNELKE-ICELTSIDQVV	319
mMyo1b RT-PCR	LERAFS	119
mMyo1b	LERAFSFRVTEAKREKVVSTTLNVAQAYYARDALAKNLYSR	360
mMyo1b	LERAFSFRVTEAKREKVVSTTLNVAQAYYARDALAKNLYSR	359
mMyo1b RT-PCR	LFSWLVNRI NESI KAQTKVRKKV MGVLDI YGFEI FEDNSF	119
mMyo1b	LFSWLVNRI NESI KAQTKVRKKV MGVLDI YGFEI FEDNSF	400
mMyo1b	LFSWLVNRI NESI KAQTKVRKKV MGVLDI YGFEI FEDNSF	399

Myo1e

mMyo1e RT-PCR	-----KPNETKKPKDWE-	1
mMyo1e ESTs	AGSKI KQKQANDLVSTLMKCTPHYRCIKPNETKKPKDWE-	14
mMyo1e	AGSKI KQKQANDLVSTLMKCTPHYRCIKPNETKKPKDWE-	600
mMyo1e RT-PCR	SRVKHQVEYLGLENIRVRRAGYARRVFOKFLQRYAII LT	41
mMyo1e ESTs	SRVKHQVEYLGLENIRVRRAGYARRVFOKFLQRYAII LT	54
mMyo1e	SRVKHQVEYLGLENIRVRRAGYARRVFOKFLQRYAII LT	640
mMyo1e RT-PCR	KATWPYWRGDEKQGVLLHLLQSVNMDSDQFQLGRSKVYFKA	81
mMyo1e ESTs	KATWPYWRGDEKQGVLLHLLQSVNMDSDQFQLGRSKVYFKA	134
mMyo1e	KATWPYWRGDEKQGVLLHLLQSVNMDSDQFQLGRSKVYFKA	680
mMyo1e RT-PCR	PESLFLLEEMREKRYDGYARVI QKTWRKVFARKKYQMR E	121
mMyo1e ESTs	PESLFLLEEMREKRYDGYARVI QKTWRKVFARKKYQMR E	134
mMyo1e	PESLFLLEEMREKRYDGYARVI QKTWRKVFARKKYQMR E	720
mMyo1e RT-PCR	EASDLL	127
mMyo1e ESTs	EASDLLLNKKERRNSINRNFI GDYI GMEERPELQQFVKG	174
mMyo1e	EASDLLLNKKERRNSINRNFI GDYI GMEERPELQQFVKG	760

Myo1g

mMyo1g RT-PCR	-----KDGFGSVLFSSHVRKYNRFRKS	22
mMyo1g ESTs	DNPTASHLFAEQLKALREKDGFGSVLFSSHVRKYNRFRKS	40
mMyo1g	DNPTASSLFAQRKTLQDKDGFSAVLFSSHVRKYNRFRK	880
mMyo1g RT-PCR	RDRALLLTDRYLKLEPGROYRVMRAVPLEAVTGLSVTS G	62
mMyo1g ESTs	RDRALLLTDRYLKLEPGROYRVMRAVPLEAVTGLSVTS G	80
mMyo1g	RDRALLLTDRYLKLEPGROYRVMRAVPLEAVTGLSVTS G	920
mMyo1g RT-PCR	RDQLVVLHAGQYDDL VVCLHRSOPPLDNRI GELVGMALAAH	102
mMyo1g ESTs	RDQLVVLHAGQYDDL VVCLHRSOPPLDNRI GELVGMALAAH	120
mMyo1g	RDQLVVLHAGQYDDL VVCLHRSOPPLDNRI GELVGMALAAH	960
mMyo1g RT-PCR	COGEGRTL EVRVSDCI PLSORGAR	126
mMyo1g ESTs	COGEGRTL EVRVSDCI PLSORGARRLISVEPRPEQPEPDF	160
mMyo1g	COGEGRTL EVRVSDCI PLSORGARRLISVEPRPEQPEPDF	1000
mMyo1g RT-PCR	QSSRSSTFTLLWPSR	126
mMyo1g ESTs	RCARGSFTLLWPSR	174
mMyo1g	RCARGSFTLLWPSR	1014

Fig. 2. Sequence analysis of mouse myosin-I transcripts. Conceptual translations of RT-PCR products were aligned with appropriate database sequences when significant differences were found or when mouse orthologs have not been previously reported. Myo1b, alignment with mouse Myo1b (myosin-1x; NM_010863) and rat Myo1b (myr 1; X68199). Myo1d, alignment with mouse Myo1d (myosin-1y; C45438) and rat Myo1d (myr 4; X71997). Myo1e, alignment with rat Myo1e (myr 3; X74815) and contiguous sequence

Myo1d

mMyo1d RT-PCR	-----YNYI RVGAQLKSS	13
mMyo1d	FHSFYQLLQGGSEQLHSLHLQKSLSSYNYI RVGAQLKSS	96
mMyo1d	FHSFYQLLQGGSEQLHSLHLQKSLSSYNYI RVGAQLKSS	240
mMyo1d RT-PCR	INDAAEFKVVADAMKVI GFKPEEIQTVYKILAAI LHLGNL	53
mMyo1d	INDAAEFKVVADAMKVI GFKPEEIQTVYKILAAI LHLGNL	136
mMyo1d	INDAAEFKVVADAMKVI GFKPEEIQTVYKILAAI LHLGNL	280
mMyo1d RT-PCR	KFIVDGDPTLIE NGKVVSVI AELLSTKADMVEKALLYRTV	93
mMyo1d	KFIVDGDPTLIE NGKVVSVI AELLSTKADMVEKALLYRTV	176
mMyo1d	KFIVDGDPTLIE NGKVVSVI AELLSTKADMVEKALLYRTV	320
mMyo1d RT-PCR	ATGRDIDKQHTEQEASY	111
mMyo1d	ATARDIDKQHTEQEASYGRDAFAKAI YERLFGWIVTRI N	216
mMyo1d	ATGRDIDKQHTEQEASYGRDAFAKAI YERLFGWIVTRI N	360
mMyo1d RT-PCR	DI IAVKKNYDITTVHGKNTVIGVLDI YGFEI FDNNSFEQFCI	111
mMyo1d	DI IAVKKNYDITTVHGKNTVIGVLDI YGFEI FDNNSFEQFCI	256
mMyo1d	DI IAVKKNYDITTVHGKNTVIGVLDI YGFEI FDNNSFEQFCI	400

Myo1f

mMyo1f RT-PCR	MGSKERFH WQSHNVKQSGVDDMVL LPIQITEDAI VSNLRKR	40
mMyo1f	MGSKERFH WQSHNVKQSGVDDMVL LPIQITEDAI VSNLRKR	96
mMyo1f	MGSKERFH WQSHNVKQSGVDDMVL LPIQITEDAI VSNLRKR	0
mMyo1f RT-PCR	FMDYYI FTYI GS VLI S VNPFF KOMPYFT DREI DLYQGAQY	80
mMyo1f	FMDYYI FTYI GS VLI S VNPFF KOMPYFT DREI DLYQGAQY	126
mMyo1f	FMDYYI FTYI GS VLI S VNPFF KOMPYFT DREI DLYQGAQY	38
mMyo1f RT-PCR	ENPPHI YALTDNMYRNM LIDCENQCVI ISGESGAGKTVA A	126
mMyo1f	ENPPHI YALTDNMYRNM LIDCENQCVI ISGESGAGKTVA A	126
mMyo1f	ENPPHI YALTDNMYRNM LIDCENQCVI ISGESGAGKTVA A	78
mMyo1f RT-PCR	KYI MGYI	127
mMyo1f	KYI MGYI SKVSGGG EKQVHV KDI ILQSNPLLEAFGNAKT V	166
mMyo1f	KYI MGYI SKVSGGG EKQVHV KDI ILQSNPLLEAFGNAKT V	118
mMyo1f RT-PCR	RNNSSRF GK YFEI QF SRGGEPDGGKI SNFLLEKSRVVMQ	127
mMyo1f	RNNSSRF GK YFEI QF SRGGEPDGGKI SNFLLEKSRVVMQ	206
mMyo1f	RNNSSRF GK YFEI QF SRGGEPDGGKI SNFLLEKSRVVMQ	150

Myo1h

mMyo1h RT-PCR	-----FVKKFIRNDKPLCPDNEEFFVVLVRKNYI	4
mMyo1h ESTs	I GYKPEEYKLGKFKGFSIRNDKPLCPDNEEFFVVLVRKNYI	34
mMyo1h	I GYKPEEYKLGKFKGFSIRNDKPLCPDNEEFFVVLVRKNYI	680
mMyo1h RT-PCR	LNLRHYHPKKNVLDKSWLRPPGILENASNLRMRMCTRNLRV R	44
mMyo1h ESTs	LNLRHYHPKKNVLDKSWLRPPGILENASNLRMRMCTRNLRV R	174
mMyo1h	LNLRHYHPKKNVLDKSWLRPPGILENASNLRMRMCTRNLRV R	720
mMyo1h RT-PCR	KYCRGISAERKAV-----MQQKVVTS EIFR	69
mMyo1h ESTs	KYCRGISAERKAV-----MQQKVVTS EIFR	99
mMyo1h	KYCRGISAERKAVKPVATIFILSI VVYQMQQKVVTS EIFR	766
mMyo1h RT-PCR	GKKEGYAESLNQIFAGSRLDESNI NPKVLQLLGSEKI QYG	106
mMyo1h ESTs	GKKEGYAESLNQIFAGSRLDESNI NPKVLQLLGSEKI QYG	135
mMyo1h	GKKEGYAESLNQIFAGSRLDESNI NPKVLQLLGSEKI QYG	800
mMyo1h RT-PCR	VPVI KYDRKGF KARORQLL	128
mMyo1h ESTs	VPVI KYDRKGF KARORQLL TORSAVVELSKVKOKIEVA	175
mMyo1h	VPVI KYDRKGF KARORQLL TORSAVVELSKVKOKIEVA	840

from mouse ESTs (Table 1). Myo1f, alignment with mouse Myo1f (NM_008660) and contiguous sequences from two human Myo1f sequences (U57053, erroneously labeled myosin-ID; X98411, erroneously labeled myosin-IE). Myo1g, alignment with human Myo1g (Berg et al. 2001) and contiguous sequence from mouse ESTs (Table 1). Myo1h, alignment with human Myo1h (Berg et al. 2001) and contiguous sequence from mouse ESTs (Table 1). Myo1a and Myo1c sequences exactly matched the database sequences.

identical to the predicted rat Myo1d sequence. Our predicted sequence for Myo1e was 99% identical to the predicted rat sequence; Myo1g was 86% identical to the predicted human Myo1g sequence. The predicted human Myo1h sequence included an addi-

tional 15 amino acids, not found in our mouse Myo1h RT-PCR product or mouse ESTs; this could represent a splicing difference. Otherwise, our mouse Myo1h sequence was 84% identical to the human sequence. These results represent the first simultaneous detec-

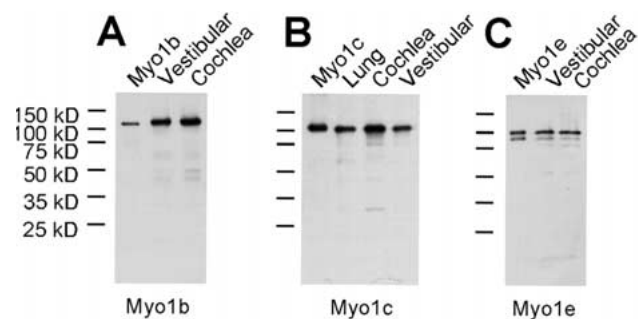


Fig. 3. Protein-immunoblot analysis of Myo1b, Myo1c, and Myo1e in rat cochlea and vestibular organs. Proteins were extracted from cochlea or vestibular organs (pooled saccules and utricles) with sample buffer and analyzed by immunoblotting. **A.** Myo1b detection; 1.9 ng Myo1b, 0.1 cochlear equivalent, and 0.5 vestibular equivalent; detection with Tü 30 antibody. **B.** Myo1c detection; 1.7 ng Myo1c, rat lung extract, 0.5 cochlear equivalent, and 0.7 vestibular equivalent; detection with R2652 antibody. **C.** Myo1e detection; 17.5 ng Myo1e, 1 cochlear equivalent, and 2 vestibular equivalents; detection with FML 6 antibody.

tion of all eight myosin-I transcripts in any species, including three (Myo1e, Myo1g, and Myo1h) previously undescribed in mouse.

Protein-immunoblot quantitation

Protein expression levels are not necessarily correlated with mRNA expression levels. We used selective antibodies, raised against rat myosin-I isozymes, to detect Myo1b, Myo1c, and Myo1e on protein immunoblots of neonatal rat cochlear and vestibular extracts (Fig. 3). A weak Myo1d band was observed by protein immunoblot analysis of cochlear (but not vestibular) extracts (data not shown). To quantify the abundance of each myosin isozyme in sensory epithelia, we used baculovirus vectors to express recombinant myosins and purified them to use as standards on immunoblots. In neonatal rat cochlea and vestibular organs, Myo1b and Myo1e were each more abundant than Myo1c (Table 2), consistent with our qualitative RT-PCR data (Fig. 1).

Myo1c in purified hair bundles

Because mouse is a good model for future molecular experiments examining mechanical transduction, and Myo1c is the likely adaptation motor for the transduction apparatus, we characterized Myo1c further in hair bundles of mouse utricles. To determine the abundance of Myo1c in hair bundles, we adapted the twist-off bundle-isolation method (Gillespie and Hudspeth 1991) to rat and mouse utricles and saccules. After adhering vestibular epithelia to glass coverslips and removing their otolithic membranes, we embedded them in molten agarose, chilled the

TABLE 2

Protein-immunoblot quantitation of myosin-I isozymes in rat inner-ear epithelia^a

Isozyme	Cochlea	Vestibular organs
Myo1b	53 ± 14 ng/cochlea (n = 3)	6 ± 3 ng/organ
Myo1c	8 ± 2	2.2 ± 0.2
Myo1e	37 ± 19	13 ± 4

^aNeonatal (P3–P5) rat cochlea or pooled vestibular organs (sacculae and utricles) were harvested and run on SDS-PAGE in parallel with recombinant myosin standards. Proteins were transferred to a blotting membrane, probed with the appropriate antibody, and visualized using chemiluminescence detection. Films were scanned and signal intensities in myosin bands were quantified with NIH Image (Scion Image version). At least three independent experiments were carried out for each isozyme.

agarose to form a stiff gel, then sheared bundles from their epithelia. With careful dissections, recoveries of bundles could exceed 90% (Fig. 4A,B), although recoveries were more typically ~50%. Using protein immunoblotting (Fig. 4C), we found that hair bundles contained 3.5 ± 1.9 pg of Myo1c per P3–P8 mouse utricle ($n = 4$). Rat vestibular bundles contained similar amounts of Myo1c (~10 pg per organ). Because we measured 1.9 ± 0.1 ng of hair-bundle actin per utricle ($n = 5$), there was one Myo1c molecule for approximately every 2300 actin molecules. Examining fixed, phalloidin-stained P5–P6 mouse utricles by confocal microscopy, we counted 2001 ± 69 ($n = 3$) hair bundles, each with 34 ± 7 ($n = 35$) stereocilia. Therefore, each stereocilium contains on average ~170 molecules of Myo1c, similar to estimates of 100–200 molecules of Myo1c per frog stereocilium (Gillespie et al. 1993; Walker and Hudspeth 1996).

Myo1b immunolocalization

Although previous experiments had demonstrated expression of Myo1b in vestibular epithelia (Solc et al. 1994), its location has not been reported. In P1 rat organ of Corti, Myo1b was enriched on apical surfaces of Deiters' cells, the supporting cells that largely surround outer hair cells (Fig. 5A, Table 3). At this developmental stage, the apical extent of the Deiters' cells was relatively large, permitting easy identification. Myo1b immunoreactivity was not observed in the organ of Corti of P7, P14, and P21 rats (Table 3).

In rat vestibular epithelia, localization of Myo1b was even more striking. Although the mosaic of supporting and hair cells is imperfectly formed at P1–P7, each hair cell contained within its apical surface a ring of Myo1b immunoreactivity (Fig. 5B, Table 3). These rings were clearly associated with circumferential actin belts of hair cells, rather than

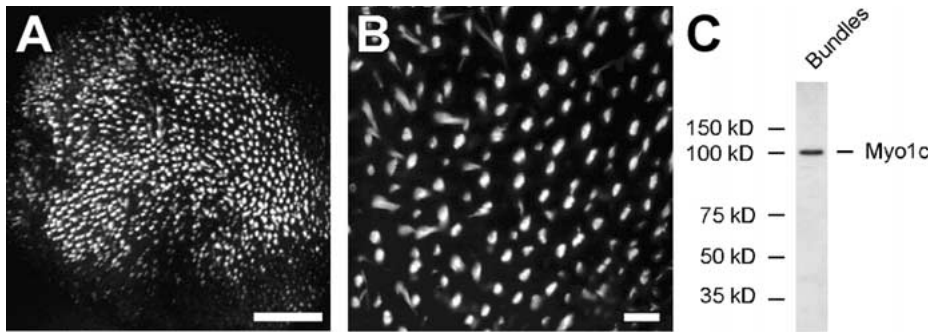


Fig. 4. Hair-bundle isolation from mouse utricle. FITC-phalloidin-labeled mouse utricular hair bundles isolated and imbedded in agarose plugs at low (A) and high (B) magnification. Scale bars: A = 100 μm ; B = 10 μm . (C) Myo1c immunoblotting of purified mouse hair bundles (8 utricle equivalents) with R2652 antibody.

the pericuticular necklace (Hasson et al. 1997). In occasional P1 samples, rings were absent and the labeling was along the apical surfaces of supporting cells (data not shown), resembling the Myo1b pattern in cochlea. Myo1b immunoreactivity was not observed in saccule or utricle in P14 and P21 rats (Table 3).

Myo1d immunolocalization

Using immunofluorescence microscopy, we did not detect expression of Myo1d in whole-mount preparations of organ of Corti or vestibular epithelia (data not shown). Because our RT-PCR data and immunoblotting data indicated that this isozyme was expressed by these epithelia, we suspect that its expression was confined to cells that were not easily accessible to the antibody using the whole-mount immunolabeling approach, or that the epitope was masked using our conditions.

Myo1e immunolocalization

Myo1e was consistently observed in the cuticular plates of both cochlear and vestibular hair cells (Fig. 5C,D, Table 3). Myo1e levels did not appear to change substantially over the P0–P21 time frame. Although cell bodies of hair cells were labeled modestly, immunoreactivity was never observed in hair bundles.

Myo1c immunolocalization

Myo1c is a candidate for the adaptation motor in frog hair cells in part because of its localization near stereocilia tips (Gillespie et al. 1993). We therefore used immunocytochemistry to determine whether localization of rodent Myo1c was similar. Because Myo1c was difficult to detect using conventional immunofluorescence methodology, we used *in situ* amplification with the biotinylated-tyramine method to gain

sufficient sensitivity (Adams 1992). Using the R2652 antibody and this method, we observed Myo1c in hair bundles of neonatal organ of Corti (Fig. 6A–D) and vestibular (Fig. 6E–J) epithelia. In the organ of Corti, Myo1c was present in both inner and outer hair cells, with relatively strong labeling in the cuticular plate and apparently uniform labeling in stereocilia. In vestibular hair cells, Myo1c was most concentrated at the stereociliary tips. Because the shortest stereocilia of rodent vestibular hair bundles are much shorter than the longest stereocilia, bright labeling often appeared to extend down to near the cuticular plate. Nevertheless, bright labeling was usually asymmetric, corresponding to the beveled edge of the bundle. Relatively little immunoreactivity was observed in somas of hair cells or supporting cells. With the amplification conditions used, control antibodies produced some labeling of hair bundles; nevertheless, immunoreactivity for Myo1c was always stronger than that for control antibodies and was located near stereociliary tips (Fig. 6E–H). By contrast, control labeling in bundles was always uniform. Myo1c labeling was observed in P1–P21 rats and mice (Table 3).

We confirmed these results with two additional preparations. We generated an additional antibody (R2695) against the C-terminal 30-kD domain of rat Myo1c and affinity-purified it against baculovirus-expressed rat T701, a fragment of rat Myo1c spanning amino acids 701–1028, coexpressed with light-chain calmodulin. Using conventional detection methods and relatively high antibody concentrations (25 $\mu\text{g}/\text{mL}$), we found intense labeling of utricle and semicircular-canal hair bundles (Fig. 6I,J). The labeling pattern in the cochlea was very similar to that seen with R2652 (e.g., Fig. 6K,L). Labeling was particularly strong with unfixed, purified hair bundles. In addition, we observed significant labeling of inner and outer-hair-cell bundles and cuticular plates (not shown). Very low labeling was seen with an irrelevant primary antibody (anti-HRP) at an

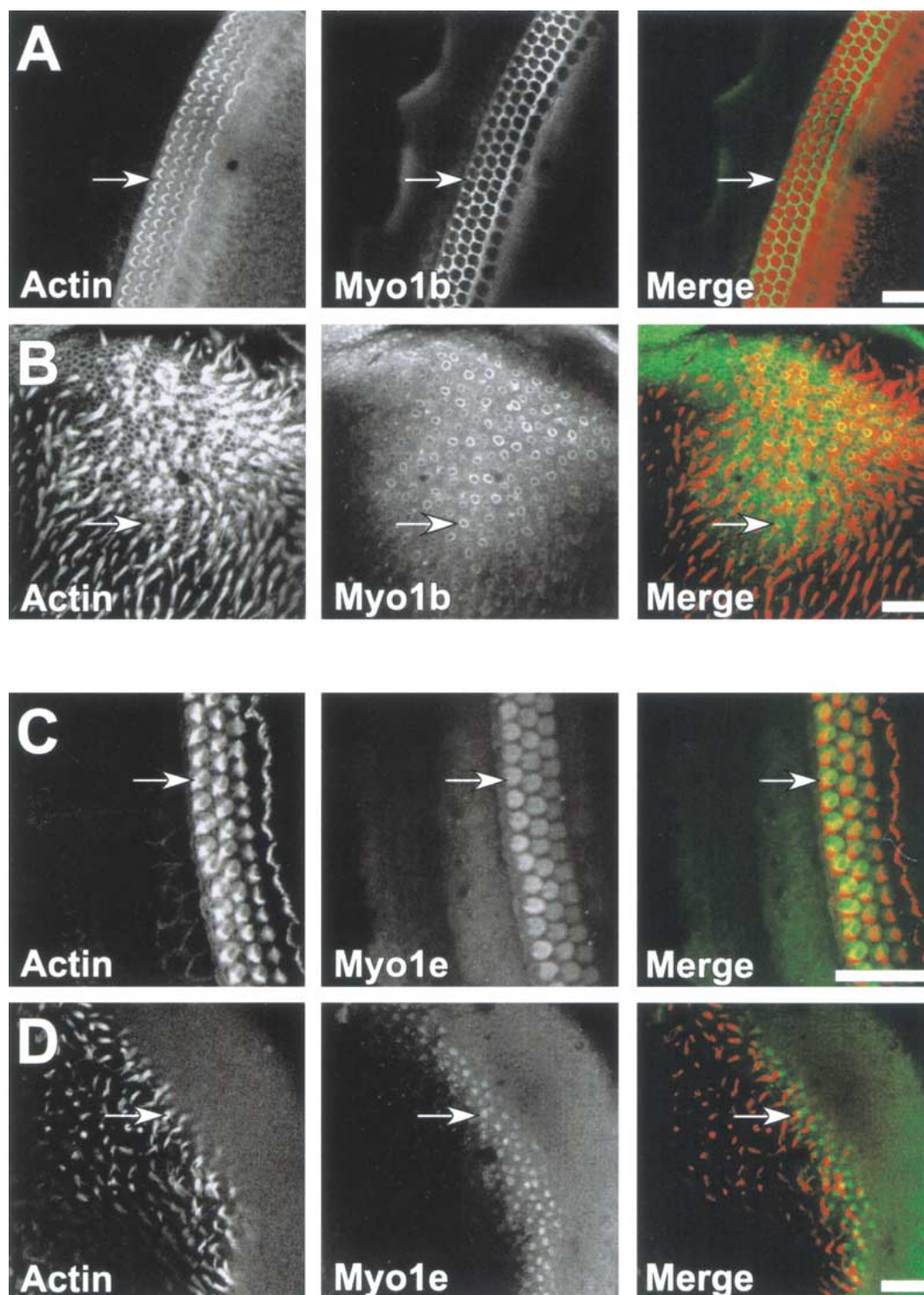


Fig. 5. Immunofluorescence localization of Myo1b and Myo1e in rat cochlea and vestibular organs. Left columns, FITC-phalloidin; middle columns, antimyosin antibody; right columns, merged phalloidin (red) and antibody (green). **A.** Myo1b immunolabeling using the Tü 30 antibody in P1 rat cochlea; arrow: labeling surrounding outer hair cell. **B.** Myo1b immunolabeling using the Tü 30

antibody in P1 rat utricle; arrow: labeling in rings associated with circumferential actin belts. **C.** Myo1e immunolabeling using the FML 6 antibody in P1 rat cochlea; arrow: labeling in outer-hair-cell cuticular plate. **D.** Myo1e immunolabeling using the FML 6 antibody in P1 rat utricle. Arrow: labeling in cuticular plate. Scale bars, 25 μm .

TABLE 3

Structure	Myosin-I localization in rodent inner-ear epithelia											
	<i>Myo1b</i>				<i>Myo1c</i>				<i>Myo1e</i>			
	P0	P7	P14	P21	P0	P7	P14	P21	P0	P7	P14	P21
<i>Cochlea</i>												
Hair bundles	-	-	-	-	+/-	+/-	+/-	+/-	-	-	-	-
Cuticular plate	-	-	-	-	+/-	+/-	+/-	+/-	+	+	+	+
ZA ring	-	-	-	-	-	-	-	-	-	-	-	-
Hair-cell body	-	-	-	-	+/-	+/-	+/-	+/-	+/-	+/-	+/-	+/-
Supporting-cell apices	++	-	-	-	-	-	-	-	-	-	-	-
Supporting-cell bodies	-	-	-	-	-	-	-	-	-	-	-	-
<i>Utricle and saccule</i>												
Hair bundles	-	-	-	-	+	+	+	+	-	-	-	-
Cuticular plate	-	-	-	-	-	-	-	-	+	+	+	+
ZA ring	++	++	-	-	-	-	-	-	-	-	-	-
Hair-cell bodies	-	-	-	-	-	-	-	-	+/-	+/-	+/-	+/-
Supporting-cell apices	+/-	-	-	-	-	-	-	-	-	-	-	-
Supporting-cell bodies	-	-	-	-	-	-	-	-	-	-	-	-

^a++, strong labeling, consistently observed; +, modest to weak labeling, consistently observed; +/-, labeling sometimes observed; -, no labeling.

identical concentration. In addition, Myo1c immunoreactivity can be more robust if fixation is avoided (Gillespie et al. 1993; Steyger et al. 1998). We therefore carried out immunocytochemistry with the R2652 antibody on unfixed, purified hair bundles. Myo1c immunoreactivity was much greater than control immunoreactivity (not shown) and was focused in a punctate fashion near stereocilia tips (Fig. 6M,N). Taken together, these diverse Myo1c immunolabeling experiments demonstrated that rodent cochlear and vestibular hair cells express Myo1c and that, at least in the vestibular system, it is concentrated at stereociliary tips.

Myo1c tail-GFP localization in hair cells

We generated an adenovirus vector (Ad-GFP::T698) that carried the gene for GFP fused, in frame, to the tail domain of Myo1c (amino acids 698–1028). To confirm targeting of Myo1c to stereociliary tips, we infected cultured hair cells of the mouse utricle with Ad-GFP::T698. GFP::T698 was targeted to hair-cell membranes, unlike GFP alone (Holt et al. 1999); in addition, levels were high in the hair bundle (Fig. 7A–D). Although we expected higher bundle fluorescence intensity because of the greater density of membrane in a confocal section, the fluorescence intensity was often particularly high at stereociliary tips (Fig. 7E,F). Tip labeling was only seen early (10–12 h) after infection; as the expression of the fusion protein increased (>24 h postinfection), GFP fluorescence patterns spread uniformly throughout the entire bundle.

DISCUSSION

Neonatal mouse utricle for molecular characterization of hair-cell transduction

Identifying the molecules responsible for mechano-transduction by hair cells has proven exceptionally difficult, in part because hair cells' scarcity has prevented straightforward biochemical and molecular biological experiments. Until recently, the experimental system best suited for molecular characterization of hair-cell transduction has not been obvious. The evidence provided here and elsewhere (Holt et al. 1997, 1999) suggests strongly that the neonatal mouse utricle is an excellent preparation. Prominent reasons for choice of this organ include the following: (1) Many mouse ESTs have been sequenced, and the mouse genome will soon be sequenced in its entirety. (2) Foreign genes can be expressed in mouse hair cells using conventional transgenic (Boeda et al. 2001), bacterial artificial chromosome transgenic (Zuo et al. 1999), or adenovirus (Holt et al. 1999) methodologies. (3) Endogenous genes of the mouse can be targeted for deletion or subtle mutagenesis (Joyner 2000). (4) Hair-cell transduction and adaptation of mouse utricle are relatively easily measured and closely resemble those in bullfrog sacculus, where they have been characterized most thoroughly (Holt et al. 1997). (5) Neonatal auditory and vestibular organs can be cultured for several days to weeks without gross morphological changes, permitting experiments of extended duration (Russell and Richardson 1987; Rusch and Eatock 1996). (6) Many cDNA libraries, DNA probes, and antibodies are available for

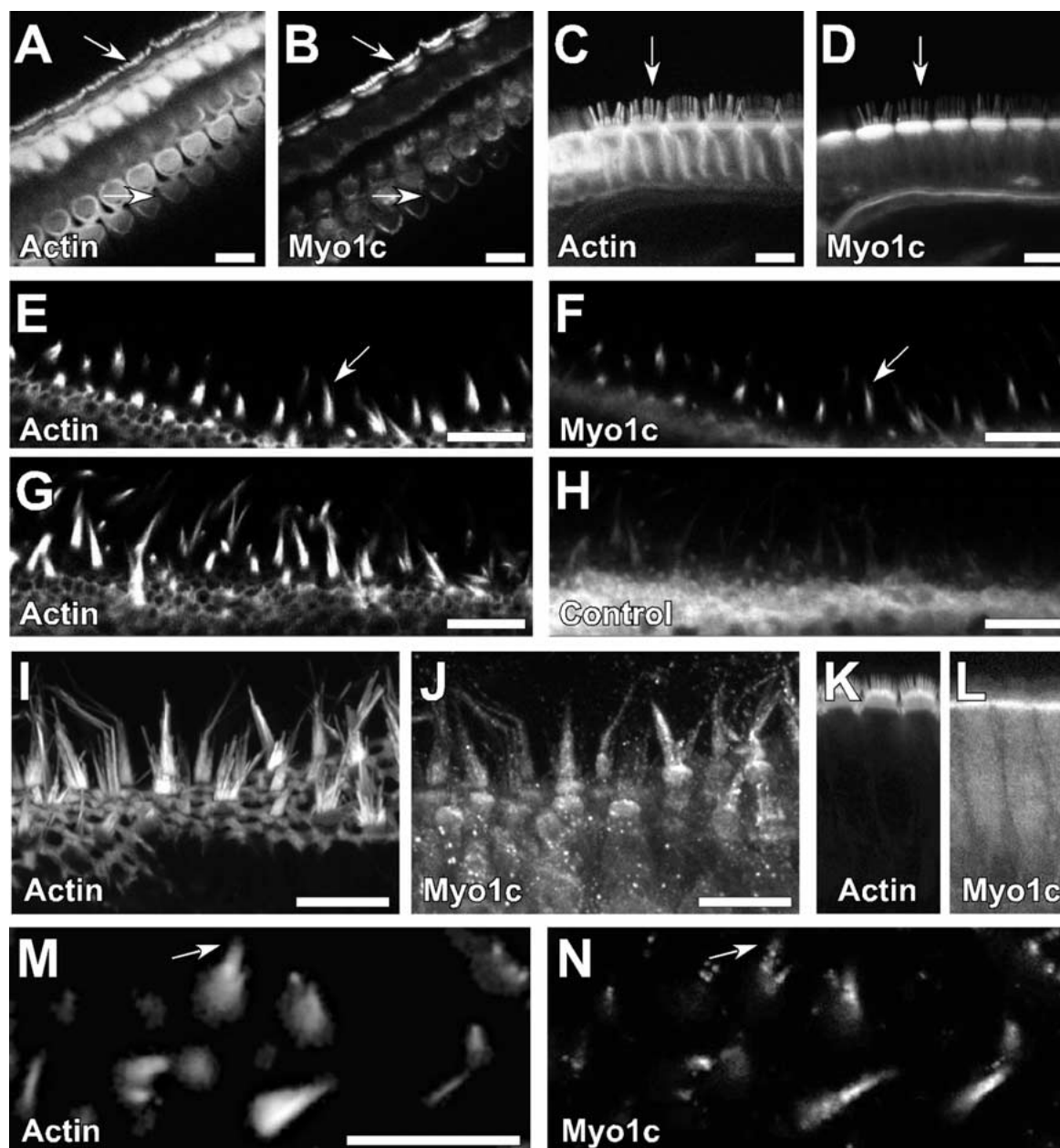


Fig. 6. Immunofluorescence localization of Myo1c in rat cochlea and vestibular organs. **A, B.** FITC-phalloidin (**A**) and Myo1c immunoreactivity using the 2652 antibody (**B**) in P14 rat cochlea. Top arrow: labeling in bundle of inner hair cell. Bottom arrow: labeling in bundle of outer hair cell. **C, D.** FITC-phalloidin (**C**) and Myo1c immunoreactivity using the 2652 antibody (**D**) in P21 rat cochlea. Arrow: labeling in bundle of inner hair cell. **E, F.** FITC-phalloidin (**E**) and Myo1c immunoreactivity using the 2652 antibody (**F**) in P7 rat vestibular organ. Arrow: labeling at tips of hair bundles. **G, H.** FITC-phalloidin (**G**) and antihorseradish peroxidase immunoreactivity (**H**)

in P7 rat vestibular organ. Samples in E–H were processed simultaneously. **I, J.** FITC-phalloidin (**I**) and Myo1c immunoreactivity using the 2695 antibody (**J**) in P7 mouse semicircular canal (projections). **K, L.** FITC-phalloidin (**K**) and Myo1c immunoreactivity using the 2695 antibody (**L**) in P7 mouse cochlea (inner hair cells). **M, N.** FITC-phalloidin (**M**) and Myo1c immunoreactivity using the 2652 antibody (**N**) in neonatal mouse vestibular hair bundles, purified, and imbedded in agarose. Arrow: note concentration of Myo1c immunoreactivity towards tips. Scale bars in panels, 10 μ m.

mouse genes, transcripts, and proteins. Here we show that hair bundles can be purified from mouse utricle in reasonable yield, permitting biochemical characterization of bundle proteins.

The organ of Corti from neonatal mice has been used extensively for characterization of properties of hair-cell transduction. Nevertheless, these hair cells are not fully developed; for example, adult innerva-

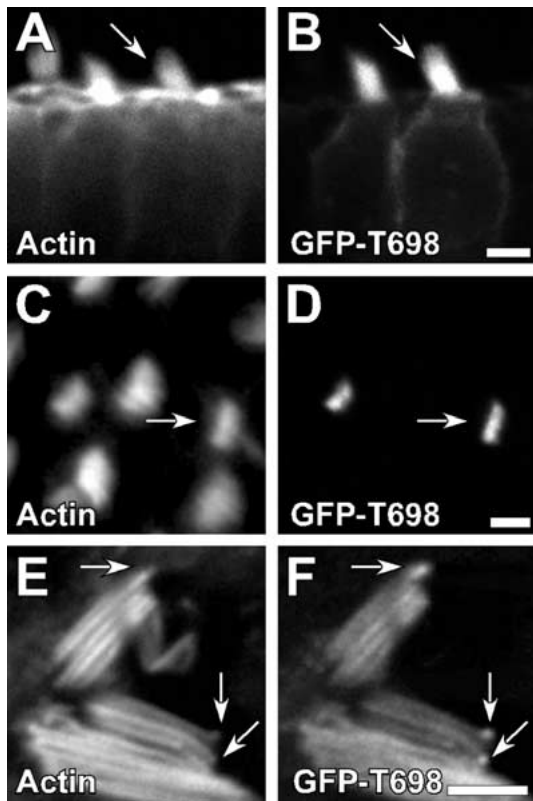


Fig. 7. Expression of GFP-Myo1c tail in mouse utricular hair cells. **A, B.** Two hair cells, shown in longitudinal section, infected with the GFP::T698 virus for 24 hours, with phalloidin-labeled actin (**A**) and GFP fluorescence (**B**). **C, D.** Two different hair cells, with the optical section near stereociliary tips, infected with the GFP::T698 virus for 24 hours, with phalloidin-labeled actin (**C**) and GFP fluorescence (**D**). **E, F.** Hair bundle viewed from above, infected with GFP::T698 virus for 12 hours, with phalloidin-labeled actin (**E**) and GFP fluorescence (**F**), bundle splayed to reveal concentration of fluorescence at tips of individual stereocilia (arrows).

tion patterns are not established until more than three weeks after birth (Sobkowicz 1992), and electromotility, thought to be essential for the sensitive operation of the cochlea, does not appear at full strength until ~P12 (Belyantseva et al. 2000). Mouse vestibular organs develop more quickly, but still not reach their fully adult form until 2–3 weeks after birth (Desmadryl et al. 1992). Nevertheless, the simplicity of dissection of the neonatal organ—transduction currents are much more easily measured—makes the neonatal mouse organ more suitable for experiments that include testing the normal function of the hair bundle.

Myosin-I isozymes in inner-ear organs

We observed by RT-PCR expression in mouse utricle all eight myosin-I isozymes. mRNA levels for Myo1b, Myo1c, and Myo1e were higher than for the other

isozymes; the corresponding three proteins were also expressed at easily detected levels. With the possible exception of Myo1d, which we detected by immunoblot in rat cochlea, and Myo1f, which has been cloned from a cochlear cDNA library (Crozet et al. 1997), expression of the other isozymes may result from basal transcription of genes not expressed at significant levels in the inner ear. Although the sensitivity of RT-PCR permits us to detect exceptionally low levels of mRNA, we suspect that little protein is expressed for each isozyme. Consistent with that interpretation, detection of Myo1a, Myo1g, and Myo1h by RT-PCR was sporadic. A possible exception might be if one or more of these isozymes is expressed at a substantial level in a scarce cell type in the inner ear.

Myo1b is prominent in auditory and vestibular epithelia for very short periods; this isozyme in each case is associated with apical structures of hair cells or supporting cells. The kinetic mechanism of rat Myo1b's actomyosin ATPase has been thoroughly characterized, and its properties suggest that this isozyme is optimized for tension maintenance (Coluccio and Geeves 1999; Veigel et al. 1999). We propose that Myo1b participates in the relative growth of apical surfaces of hair and supporting cells. Consistent with this interpretation, Myo1b is particularly enriched in cellular protrusions of cultured cells, including lamellopodia, membrane ruffles, and filopodia (Ruppert et al. 1995). Indeed, Myo1b may participate directly in dynamic properties of motile cells at their leading edges (Tang and Ostap 2001). Notably, apical surfaces of Deiters' cells—the location of Myo1b in the organ of Corti—are densely packed with microvilli immediately after birth, but largely lose these microvilli by day 10 (Lim and Anniko 1985). If these microvilli are involved in transport of nutrients during organ of Corti development, as are microvilli of the intestinal epithelium, Myo1b may play a role in transport as has been proposed for Myo1a in the intestine (Skowron and Mooseker 1999).

Myo1e is localized to cuticular plates of hair cells, which consist of a meshwork of crosslinked actin filaments (DeRosier and Tilney 1989); significantly, rat Myo1e (myr 3) crosslinks actin filaments (Stoffler and Bähler 1998), suggesting that Myo1e may share this role in hair cells with Myo6, which has also been proposed to crosslink cuticular-plate actin filaments (Hasson et al. 1997). The ATPase activity of Myo1e is regulated by its own tail domain, including its SH3 domain (Stoffler and Bähler 1998), suggesting that a binding partner may control its activity and hence the actin crosslinking properties. In other cells, Myo1e is concentrated on actin-rich structures containing alpha-actinin (Stoffler et al. 1995); notably, cuticular

plates of mammalian hair cells contain substantial amounts of alpha-actinin (Slepecky and Chamberlain 1985; Slepecky and Ulfendahl 1992). Although MyoIe localizes in many cell types to adheren junctions (Stoffler et al. 1995, 1998), we did not observe this isozyme in such junctions of hair cells. We suggest that one role for MyoIe in hair cells may be to control tension of actin filaments within the cuticular plate, under unknown control.

Myosin-Ic and adaptation

As in bullfrog sacculus Gillespie and Hudspeth 1993; Metcalf et al. 1994; Solc et al. 1994; Hasson et al. 1997), MyoIc is the best candidate for the adaptation motor in rat and mouse utricle. MyoIe is localized near stereociliary tips, the site of adaptation, and is present in sufficient quantity (~170 molecules per stereocilium) to fulfill the need for substantial force generation, minimization of transduction-current noise generated by motor stepping, and continuous attachment (Hudspeth and Gillespie 1994; Gillespie and Corey 1997). These data support our demonstration that inhibition of a nucleotide-sensitized MyoIc mutant produces a block of adaptation, strongly implicating MyoIc as the adaptation motor (Holt et al. 2001).

All myosin-I isozymes have a highly basic tail segment, which targets myosin to acidic phospholipids. Protein expressed by the T698-GFP adenovirus construct is enriched in hair bundles, perhaps because the bundle is rich in phosphatidylinositol bisphosphate (Tachibana et al. 1984). When expression levels are low, T698-GFP first binds near stereociliary tips; as expression levels rise, the localization domain expands to include the entire hair-bundle membrane. T698-GFP presumably interacts with MyoIc receptors, which should be located at stereociliary tips to organize the adaptation-motor myosins (Gillespie and Corey 1997). As with other myosin isozymes, however, the motor head domain may also be necessary to properly target MyoIc (Tang and Ostap 2001).

The role of MyoIc in cochlear hair cells is less clear. Although antibodies detected MyoIc in inner and outer hair cells, this isozyme was not obviously concentrated at stereociliary tips. Because prominent slow adaptation is generally not apparent in cochlear hair cells (Kros et al. 1992; Geleoc et al. 1997), these hair cells may not require an adaptation motor. Nevertheless, the adaptation motor may play other essential roles besides mediating slow adaptation, including setting the resting tension applied to the transduction channels (Gillespie and Corey 1997; Steyger et al. 1998; Gillespie and Walker 2001). Al-

ternatively, maintenance of resting tension may be set in cochlear hair cells by another isozyme, such as myosin-VIIa (Kros et al. 2002).

ACKNOWLEDGMENTS

We thank Jonathan Berg and Richard Cheney for sharing human MyoIg and MyoIh sequences and for nomenclature discussions. We also thank Susan Gillespie for comments on the manuscript. This study was supported by NIH grants DC02368 and DC03279. J.R.H. was supported by an NIDCD grant (DC00304) to D.P. Corey, an Investigator with the Howard Hughes Medical Institute. The GenBank accession numbers for sequences reported here are AF426463 (MyoIb), AF426464 (MyoId), AF426465 (MyoIe), AF426466 (MyoIf), AF426468 (MyoIg), and AF426467 (MyoIh).

REFERENCES

- ADAMS JC. Biotin amplification of biotin and horseradish peroxidase signals in histochemical stains. *J. Histochem. Cytochem.* 40:1457–1463, 1992.
- ALTSCHUL SF, GISH W, MILLER W, MYERS EW, LIPMAN DJ. Basic local alignment search tool. *J. Mol. Biol.* 215:403–410, 1990.
- AVRAHAM KB, HASSON T, STEEL KP, KINGSLEY DM, RUSSELL LB. The mouse Snell's waltzer deafness gene encodes an unconventional myosin. *Nat. Genet.* 11:369–375, 1995.
- BÄHLER M, KROSCHEWSKI R, STOFFLER HE, BEHRMANN T. Rat myt 4 defines a novel subclass of myosin I: identification, distribution, localization, and mapping of calmodulin-binding sites with differential calcium sensitivity. *J. Cell Biol.* 126:375–389, 1994.
- BELYANTSEVA IA, ADLER HJ, CURI R, FROLENKOV GI, KACHAR B. Expression and localization of prestin and the sugar transporter GLUT-5 during development of electromotility in cochlear outer hair cells. *J. Neurosci.* 20:RC116, 2000.
- BERG JS, POWELL BC, CHENEY RE. A millennial myosin census. *Mol. Biol. Cell* 12:780–794, 2001.
- BOEDA B, WEIL D, PETIT C. A specific promoter of the sensory cells of the inner ear defined by transgenesis. *Hum. Mol. Genet.* 10:1581–1589, 2001.
- BURLACU S, TAP WD, LUMPKIN EA, HUDSPETH, AJ. ATPase activity of myosin in hair bundles of the bullfrog's sacculus. *Biophys. J.* 72:263–271, 1997.
- COLUCCIO LM. Myosin I. *Am. J. Physiol.* 273:C347–359, 1997.
- COLUCCIO LM, GEEVES MA. Transient kinetic analysis of the 130-kDa myosin I (MYR-1 gene product) from rat liver. A myosin I designed for maintenance of tension? *J. Biol. Chem.* 274:21575–21580, 1999.
- CROZET F, EL AMRAOUI A, BLANCHARD S, LENOIR M, RIPPOLL C, VAGO P, HAMEL C, FIZAMES C, LEVI-ACOBAS F, DEPETRIS D, MATTEI MG, WEIL D, PUJOL R, PETIT C. Cloning of the genes encoding two murine and human cochlear unconventional type I myosins. *Genomics* 40:332–341, 1997.
- DEROSIER DJ, TILNEY LG. The structure of the cuticular plate, an *in vivo* actin gel. *J. Cell Biol.* 109:2853–2867, 1989.
- DESMADRYL G, DECHESNE CJ, RAYMOND J. Recent aspects of development of the vestibular sense organs and their innervation. In: Romand R (ed) *Development of the Auditory and Vestibular Systems 2*. Amsterdam, Elsevier, pp 461–487, 1992.

- DRENCKHAHN D, ENGEL K, HÖFER D, MERTE C, TILNEY L, TILNEY M. Three different actin filament assemblies occur in every hair cell: each contains a specific actin crosslinking protein. *J. Cell Biol.* 112:641–651, 1991.
- GARCIA JA, YEE AG, GILLESPIE PG, COREY DP. Localization of myosin- $I\beta$ near both ends of tip links in frog saccular hair cells. *J. Neurosci.* 18:8637–8647, 1998.
- GELLEOC GS, LENNAN GW, RICHARDSON GP, KROS CJ. A quantitative comparison of mechano-electrical transduction in vestibular and auditory hair cells of neonatal mice. *Proc. R. Soc. B Biol. Sci.* 264:611–621, 1997.
- GIBSON F, WALSH J, MBURU P, VARELA A, BROWN KA, ANTONIO M, BEISEL KW, STEEL KP, BROWN SDM. A type VII myosin encoded by the mouse deafness gene shaker-1. *Nature* 374:62–64, 1995.
- GILLESPIE PG, ALBANESI JP, BÄHLER M, BEMENT WM, BERG JS, BURGESS DR, BURNSIDE B, CHENEY RE, COREY DP, COUDRIER E, et al. Myosin-I nomenclature. *J. Cell Biol.* 155:703–704, 2001.
- GILLESPIE PG, COREY DP. Myosin and adaptation by hair cells. *Neuron* 19:955–958, 1997.
- GILLESPIE PG, GILLESPIE SK. Improved electrophoresis and transfer of picogram amounts of protein with hemoglobin. *Anal. Biochem.* 246:239–245, 1997.
- GILLESPIE PG, GILLESPIE SK, MERCER JA, SHAH K, SHOKAT KM. Engineering of the myosin- $I\beta$ nucleotide-binding pocket to create selective sensitivity to N^6 -modified ADP analogs. *J. Biol. Chem.* 274:31373–31381, 1999.
- GILLESPIE PG, HASSON T, GARCIA JA, COREY DP. Multiple myosin isozymes and hair-cell function. *Cold Spring Harb. Symp. Quant. Biol.* 61:309–318, 1996.
- GILLESPIE PG, HUDSPETH AJ. High-purity isolation of bullfrog hair bundles and subcellular and topological localization of constituent proteins. *J. Cell Biol.* 112:625–640, 1991.
- GILLESPIE PG, HUDSPETH AJ. Adenine nucleoside diphosphates block adaptation of mechano-electrical transduction in hair cells. *Proc. Natl. Acad. Sci. USA* 90:2710–2714, 1993.
- GILLESPIE PG, WAGNER MC, HUDSPETH AJ. Identification of a 120 kd hair-bundle myosin located near stereociliary tips. *Neuron* 11:581–594, 1993.
- GILLESPIE PG, WALKER RG. Molecular basis of mechanosensory transduction. *Nature* 413:194–202, 2001.
- HASSON T, GILLESPIE PG, GARCIA JA, MACDONALD RB, ZHAO Y, YEE AG, COREY DP. Unconventional myosins in inner-ear sensory epithelia. *J. Cell Biol.* 137:1287–1307, 1997.
- HOLLEY MC, KALINEC F, KACHAR B. Structure of the cortical cytoskeleton in mammalian outer hair cells. *J. Cell Sci.* 102:569–580, 1992.
- HOLT JR, COREY DP, EATOCK RA. Mechano-electrical transduction and adaptation in hair cells of the mouse utricle, a low-frequency vestibular organ. *J. Neurosci.* 17:8739–8748, 1997.
- HOLT JR, GILLESPIE SKH, PROVANCE DW, SHAH K, SHOKAT KM, COREY DP, MERCER JA, GILLESPIE PG. A chemical-genetic strategy demonstrates myosin 1c mediates adaptation by hair cells. *Cell* 108:371–381, 2002.
- HOLT JR, JOHNS DC, WANG S, CHEN ZY, DUNN RJ, MARBAN E, COREY DP. Functional expression of exogenous proteins in mammalian sensory hair cells infected with adenoviral vectors. *J. Neurophysiol.* 81:1881–1888, 1999.
- HUDSPETH AJ, GILLESPIE PG. Pulling springs to tune transduction: adaptation by hair cells. *Neuron* 12:1–9, 1994.
- JOYNER AL. *Gene Targeting: A Practical Approach*. Oxford, Oxford University Press, 2000.
- KROS CJ, MARCOTTI W, VAN NETTEN SM, SELF TJ, LIBBY RT, BROWN SDM, RICHARDSON GP, STEEL KP. Reduced climbing and increased slipping adaptation in cochlear hair cells of mice with mutations in the *Myo7a* gene. *Nat. Neurosci.* 5:41–47, 2002.
- KROS CJ, RÜSCH A, RICHARDSON GP. Mechano-electrical transducer currents in hair cells of the cultured neonatal mouse cochlea. *Proc. R. Soc. Lond. B Biol. Sci.* 249:185–193, 1992.
- LALWANI AK, GOLDSTEIN JA, KELLEY MJ, LUXFORD W, CASETELEIN CM, MHATRE AN. Human nonsyndromic hereditary deafness DFNA17 is due to a mutation in nonmuscle myosin MYH9. *Am. J. Hum. Genet.* 67:1121–1128, 2000.
- LIM DJ, ANNIKO M. Development morphology of the mouse inner ear. A scanning electron microscopic observation. *Acta Otolaryngol. Suppl.* 422:1–69, 1985.
- METCALF AB, CHELLIAH Y, HUDSPETH AJ. Molecular cloning of a myosin $I\beta$ isozyme that may mediate adaptation by hair cells of the bullfrog's internal ear. *Proc. Natl. Acad. Sci. USA* 91:11821–11825, 1994.
- O'REILLY DR, MILLER LK, LUCKOW VA. *Baculovirus Expression Vectors: A Laboratory Manual*. New York, Oxford University Press, 1994.
- PROBST FJ, FRIDELL RA, RAPHAEL Y, SAUNDERS TL, WANG A, LIANG Y, MORELL RJ, TOUCHMAN JW, LYONS RH, NOBEN-TRAUTH K, FRIEDMAN TB, CAMPER SA. Correction of deafness in shaker-2 mice by an unconventional myosin in a BAC transgene. *Science* 280:1444–1447, 1998.
- RUPPERT C, GODEL J, MULLER RT, KROSCHEWSKI R, REINHARD J, BÄHLER M. Localization of the rat myosin I molecules myr 1 and myr 2 and in vivo targeting of their tail domains. *J. Cell Sci.* 108:3775–3786, 1995.
- RUPPERT C, KROSCHEWSKI R, BÄHLER M. Identification, characterization and cloning of myr 1, a mammalian myosin-I. *J. Cell Biol.* 120:1393–1403, 1993.
- RUSCH A, EATOCK RA. A delayed rectifier conductance in type I hair cells of the mouse utricle. *J. Neurophysiol.* 76:995–1004, 1996.
- RUSSELL IJ, RICHARDSON GP. The morphology and physiology of hair cells in organotypic cultures of the mouse cochlea. *Hear. Res.* 31:9–24, 1987.
- SHERR EH, JOYCE MP, GREENE LA. Mammalian myosin I α , I β , and I γ : new widely expressed genes of the myosin I family. *J. Cell Biol.* 120:1405–1416, 1993.
- SKOWRON JF, MOOSEKER MS. Cloning and characterization of mouse brush border myosin-I in adult and embryonic intestine. *J. Exp. Zool.* 283:242–257, 1999.
- SLEPECKY NB, CHAMBERLAIN SC. Immunoelectron microscopic and immunofluorescent localization of cytoskeletal and muscle-like contractile proteins in inner ear sensory hair cells. *Hear. Res.* 20:245–260, 1985.
- SLEPECKY NB, ULFENDAHL M. Actin-binding and microtubule-associated proteins in the organ of Corti. *Hear. Res.* 57:201–215, 1992.
- SOBKOWICZ HA. The development of innervation in the organ of Corti. In: Romand R (ed). *Development of the Auditory and Vestibular Systems 2*. Amsterdam, Elsevier, pp 59–100, 1992.
- SOLC CK, DERFLER BH, DUYK GM, COREY DP. Molecular cloning of myosins from bullfrog saccular macula: a candidate for the hair cell adaptation motor. *Aud. Neurosci.* 1:63–75, 1994.
- STEYGER PS, GILLESPIE PG, BAIRD RA. Myosin $I\beta$ is located at tip link anchors in vestibular hair bundles. *J. Neurosci.* 18:4603–4615, 1998.
- STOFFLER HE, BÄHLER M. The ATPase activity of Myr3, a rat myosin I, is allosterically inhibited by its own tail domain and by Ca^{2+} binding to its light chain calmodulin. *J. Biol. Chem.* 273:14605–14611, 1998.
- STOFFLER HE, HONNERT U, BAUER CA, HOFER D, SCHWARZ H, MULLER RT, DRENCKHAHN D, BÄHLER M. Targeting of the myosin-I myr 3 to intercellular adherens type junctions induced by dominant active Cdc42 in HeLa cells. *J. Cell Sci.* 111:2779–2788, 1998.
- STOFFLER HE, RUPPERT C, REINHARD J, BÄHLER M. A novel mammalian myosin I from rat with an SH3 domain localizes to Con A-

inducible, F-actin-rich structures at cell-cell contacts. *J. Cell Biol.* 129:819–830, 1995.

- TACHIBANA M, MORIOKA H, MACHINO M, OSHIMA W, MIZUKOSHI F, MIZUKOSHI O, YOSHIOKA T. Localization of triphosphoinositide in the cochlea. An electronmicroscopic immunocytochemical study. *Histochemistry* 81:157–160, 1984.
- TANG N, OSTAP EM. Motor domain-dependent localization of Myo1b (*myr-1*). *Curr. Biol.* 11:1131–1135, 2001.
- VIEGEL C, COLUCCIO LM, JONTES JD, SPARROW JC, MILLIGAN RA, MOLLOY JE. The motor protein myosin-I produces its working stroke in two steps. *Nature* 398:530–533, 1999.

WALKER RG, HUDSPETH AJ. Calmodulin controls adaptation of mechano-electrical transduction by hair cells of the bullfrog's sacculus. *Proc. Natl. Acad. Sci. USA* 93:2203–2207, 1996.

YAMOAH EN, GILLESPIE PG. Phosphate analogs block adaptation in hair cells by inhibiting adaptation-motor force production. *Neuron* 17:523–533, 1996.

ZUO J, TREADAWAY J, BUCKNER TW, FRITZSCH B. Visualization of $\alpha 9$ acetylcholine receptor expression in hair cells of transgenic mice containing a modified bacterial artificial chromosome. *Proc. Natl. Acad. Sci. USA*. 96:14100–14105, 1999.